Double layer of Platinum Electrodes: Non-Monotonic Surface Charging Phenomena and Negative Double Layer Capacitance

Jun Huang,[a,†] Tao Zhou,[a] Jianbo Zhang,[b] Michael Eikerling[c,†]

[a] College of Chemistry and Chemical Engineering, Central South University, Changsha 410083, P.R. China.
[b] Department of Automotive Engineering, State Key Laboratory of Automotive Safety and Energy, Tsinghua University, Beijing 100084, China
[c] Department of Chemistry, Simon Fraser University, Burnaby, BC V5A 1S6, Canada

† Corresponding authors: meikerl@sfu.ca (M. Eikerling), jhuangelectrochem@qq.com (J. Huang)

Abstract

In this study, the refined double layer model of platinum electrodes accounts for chemisorbed oxygen species, oriented interfacial water molecules and ion size effects in solution. It results in a non-monotonic surface charging relation and a peculiar capacitance vs. potential curve with a maximum and maybe negative-defined values in the potential regime of oxide-formation.

Keywords

Pt electrocatalysis; surface charging effects; double layer capacitance; surface oxide dipole

1

Introduction

The surface charging relation of a metal electrode is of paramount importance in electrochemistry.[1, 2] It dictates electrostatic interactions between the charged interface and ions in solution, and thus governs local reaction conditions at the reaction plane. Thereby, the surface charging relation determines the activity and stability of electrochemical interface. Historically, the potential of zero charge (pzc), coined by A.N. Frumkin[3] and termed as one of the most fundamental ideas in electrochemistry,[2] has been employed to describe the surface charging relation,[4, 5] which is usually written as,

$$\sigma^M = C_{\mathrm{dl}}\left(\phi^M - \phi_{\mathrm{pzc}}\right). \tag{1}$$

In Eq.(1), the double-layer capacitance C_{dl} is usually considered to be a positive-defined and weakly dependent function of the electrode potential, ϕ^{M}, resulting in a monotonic relation between σ^M and ϕ^{M}.

However, for a Pt electrode, classical radiotracer experiments of Frumkin and Petrii[4] and more recent laser-pulsed experiments of Garcia-Araez et al.[6] have revealed a peculiar non-monotonic charging behaviour with consecutive transitions from negative to positive and further to negative surface charge density as ϕ^{M} is increased from the hydrogen adsorption region to the region of surface oxide formation. This alternating charging behaviour implies that the pzc is an oversimplified concept to describe metal surface charging phenomena in a wide potential range. Therefore, we must go beyond the pzc concept and scrutinize the metal charging relation from first-principles.

As discussed in a recent perspective article,[7] the development of fully-fletched DFT-based methodologies to self-consistently describe electrochemical interfaces will remain a foremost albeit highly ambitious goal in theoretical electrocatalysis for the foreseeable future. In the interim and as the foundation for further computational forays, a viable theoretical methodology of surface charging effects is needed that minimizes the required input from explicit DFT calculations. We have developed and presented a theoretical framework for Pt electrodes that accounts explicitly for the impacts of chemisorbed oxygen species and oriented surficial water molecules.[8] The model reproduces the negative-positive-negative sequence of transitions in surface charge density. It attributes the negative surface charge density region at high ϕ^M to the surface dipole moment exerted by chemisorbed oxygen that is formed at the Pt surface.

The previous model employed the classical Poisson-Boltzmann (PB) equation of point ions to account for distributions of ions and electrostatic potential in solution.[8] However, the simple PB equation becomes inadequate to describe the electrified interface at high surface charge density or in concentrated solution, such as realized in ionic liquids.[9-12] Therefore, in the present study, we amend the previous model by adopting the modified PB equation, that was introduced by Bikerman[13] and reformulated thereafter by several authors,[9-12] to account for the ion size effect. Moreover, the differential double layer capacitance C_{dl}, defined as $\partial\sigma^M/\partial\phi^M$, is derived and discussed in this study. C_{dl} can be measured using electrochemical impedance spectroscopy (EIS).[14-16] For practical uses in porous electrode models, the relation $C_{dl} = f(\phi^M)$ can be employed to parameterize the charging response of the electrified

interfaces. In addition, two key parameters of the previous model are modified based on more recent DFT calculations.

Theory development

The structural model for the Pt-solution interface is schematically illustrated in Figure 1. It consists of (i) a diffuse layer stretching towards the bulk solution;[17, 18] (ii) an outer Helmholtz plane (OHP), at which the closest counter-ions are rigidly lined up;[19, 20] (iii) an inner Helmholtz plane (IHP), at which interfacial water molecules[21] and solvated adsorbed species locate; and (iv) a layer of chemisorbed oxygen species on the metal surface. The global variables that control the configurational structure of these layers are ϕ^M and the solution pH. The electrolyte solution contains ionic species C^+, A^-, H^+, and OH^-, with bulk concentrations $c_{\text{tot}} - c_{H^+}^{\text{bulk}}$, $c_{\text{tot}} - c_{OH^-}^{\text{bulk}}$, $c_{H^+}^{\text{bulk}}$, $c_{OH^-}^{\text{bulk}}$, respectively, where c_{tot} is the total ionic concentration.

The self-consistent theory of charging phenomena at the Pt-solution interface (i) unveils the correlation between properties of the layer of chemisorbed oxygen species and ϕ^M as well as pH; (ii) provides an explicit analytical expression of the surface charging relation; and (iii) gives analytical expressions and deconvolution of the double layer capacitance. Two crucial conditions must be imposed to obtain a closed-form expression for σ^M as a function of ϕ^M and solution properties: (i) the potential gradient at the OHP is related to the free charge density on the electrode surface, σ^M, and (ii) the potential must be continuous from the interior of the metal to the bulk solution phase.

The model is mean-field. Admittedly a mean-field treatment of nanoscale phenomena has its fundamental limitations. Notwithstanding, it fulfils our goal of achieving a qualitative understanding of surface charging behaviour at Platinum electrodes. In what follows, we present modifications and new developments of the Pt-solution interface model, and refer interested readers to our previous work[8] for other information that has been introduced before.
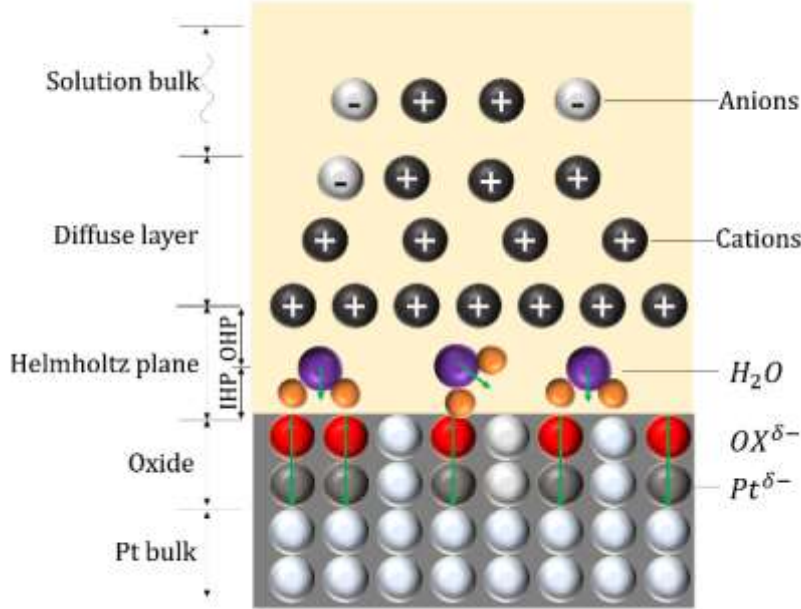

Figure 1. Structural schematic of the Pt-solution interface.

On the solution side, the distribution of dimensionless potential, $\widetilde{\phi}^S = (\phi^S - \phi_{bulk}^S)F/RT$, with the gas constant R, the temperature T, the Faraday constant F and the bulk solution potential ϕ_{bulk}^S, is described by the modified PB equation,[12]

$$\frac{\partial^2 \widetilde{\phi}^S}{\partial \widetilde{x}^2} = \frac{\sinh(\widetilde{\phi}^S)}{1 + 2\gamma \sinh^2\left(\frac{\widetilde{\phi}^S}{2}\right)},$$

(2)

where $\gamma = 2c_{tot}/c_{max}$ with c_{max} being the maximal possible local concentration of ions (both cations and anions) is termed as the compacity, $\tilde{x} = x/\lambda_D$ is the dimensionless coordinate with $\lambda_D = \sqrt{\epsilon^S RT/2F^2 c_{tot}}$ being the Debye length, ϵ^S is the dielectric constant of the solution. Here, solvent molecules are treated implicitly using a primitive model, namely the solvent effect is accounted for by the use of ϵ^S. Eq.(2) is reduced to the simple PB equation when $\gamma = 0$, namely an infinitely dilute case.

The boundary conditions to close Eq.(2) are: (i) at the OHP, $\tilde{x} = 0$,

$$\nabla\widetilde{\phi}^S = -\tilde{\sigma}^M, \tag{3}$$

where $\tilde{\sigma}^M = F\lambda_D\sigma^M/RT\epsilon^S$ is the dimensionless surface free charge density; and (ii) in the bulk solution phase at infinite distance, $\tilde{x} = \infty$,

$$\nabla\widetilde{\phi}^S = 0, \widetilde{\phi}^S = 0. \tag{4}$$

Solving Eq.(2) leads to the expression for potential at the OHP, ϕ_{OHP},

$$\phi_{OHP} = \text{sign}(\tilde{\sigma}^M)\frac{2RT}{F} \times \text{arsinh}\left(\sqrt{\frac{\exp\left(\frac{\gamma}{2}(\tilde{\sigma}^M)^2\right) - 1}{2\gamma}}\right), \tag{5}$$

where $\text{sign}(\tilde{\sigma}^M) = 1$ for $\tilde{\sigma}^M > 0$ and $\text{sign}(\tilde{\sigma}^M) = -1$ for $\tilde{\sigma}^M < 0$.

On the other hand, ϕ_{OHP} can be calculated from the metal side,[8]

$$\phi_{OHP} = \phi^M - \Delta\phi^M - \frac{\mu_{PtO}}{\epsilon_{PtO}} + \frac{N_{tot}\mu_w}{\epsilon_{IHP}}\tanh(X) - \sigma^M\left(\frac{\delta_{OHP}}{\epsilon_{OHP}} + \frac{\delta_{IHP}}{\epsilon_{IHP}}\right), \tag{6}$$

where $\Delta\phi^M$ is the constant potential drop at the metal surface due to electron spillover,[22] ϵ_{PtO} the dielectric constant of the oxide layer, μ_w the water dipole moment, δ_{OHP} the thickness of the

6

OHP, ϵ_{OHP} the dielectric constant of the OHP, δ_{IHP} the thickness of the IHP, ϵ_{IHP} the dielectric constant of the IHP.

The effective surficial oxide dipole moment μ_{PtO} is approximated by a linear relation,[23]

$$\mu_{\text{PtO}} = N_{\text{tot}}(\theta_{\text{OX}} \times \varsigma e \times \delta_{\text{PtO}}), \tag{7}$$

with N_{tot} being the surface atom density, ς the average charge number of Pt and $O_{\text{ad}}/OH_{\text{ad}}$ atoms, which can be determined from DFT,[23] and θ_{OX} being the normalized coverage of chemisorbed oxygen species, which is a function of ϕ^M and pH, as expressed in Eq.(5) in ref 8.

The variable X represents the dimensionless total field-dependent adsorption energy of interfacial water molecules, which is found from the following relation,[8, 24]

$$\left(\frac{0.6}{\pi \delta_{\text{IHP}}^2} + N_{\text{tot}} \right) \frac{N_A \mu_w^2}{\delta_{\text{IHP}} \epsilon_{\text{IHP}} RT} \tanh(X) - X = \frac{N_A \mu_w \sigma^M}{\epsilon_{\text{IHP}} RT}, \tag{8}$$

with Avogadro's number N_A. Here, we assume that only one water molecule adsorbs on one Pt site.

Combining Eq.(5) and (6) leads to a novel metal charging relation derived from the refined structural model of Pt-solution interface,

$$\begin{aligned} \text{sign}(\tilde{\sigma}^M) \frac{2RT}{F} \text{arsinh} & \left(\sqrt{\frac{1}{2\gamma} \left(\exp\left(\frac{\gamma}{2} (\tilde{\sigma}^M)^2 \right) - 1 \right)} \right) \\ & + \sigma^M \left(\frac{\delta_{\text{OHP}}}{\epsilon_{\text{OHP}}} + \frac{\delta_{\text{IHP}}}{\epsilon_{\text{IHP}}} \right) \\ & = (\phi^M - \phi_{bulk}^S) - \Delta\phi^M - \frac{\mu_{\text{PtO}}}{\epsilon_{\text{PtO}}} + \frac{N_{\text{tot}} \mu_w}{\epsilon_{\text{IHP}}} \tanh(X). \end{aligned} \tag{9}$$

Eq.(9) reduces to,

$$\frac{2RT}{F}\text{arsinh}\left(\frac{F\lambda_D\sigma^M}{2RT\epsilon^S}\right) + \sigma^M\left(\frac{\delta_{\text{OHP}}}{\epsilon_{\text{OHP}}} + \frac{\delta_{\text{IHP}}}{\epsilon_{\text{IHP}}}\right)$$

$$= (\phi^M - \phi^S_{bulk}) - \Delta\phi^M - \frac{\mu_{\text{PtO}}}{\epsilon_{\text{PtO}}} + \frac{N_{\text{tot}}\mu_{\text{w}}}{\epsilon_{\text{IHP}}}\tanh(X), \tag{10}$$

for $\gamma \to 0$ corresponding to an infinitely dilute solution. Surface charging relations derived from Bockris and Gouy-Chapman-Stern (GCS) model are given in the appendix. Note that both Bockris and GCS model are modified by taking into account the ion size effect in this paper.

Using $C_{\text{dl}} = \partial\sigma^M/\partial\phi^M$, an expression for the double layer capacitance can be deduced, which is given by,

$$C_{\text{dl}} = C_{dl}^{\text{Bockris}}(1 - \chi_{\text{OX}}), \tag{11}$$

where χ_{OX} is a coefficient accounting for the effect of chemisorbed oxygen species formation on C_{dl},

$$\chi_{\text{OX}} = \frac{N_{\text{tot}} \times \varsigma e \times \delta_{\text{PtO}}}{\epsilon_{\text{PtO}}}\frac{F\theta_{\text{OX}}(1 - \theta_{\text{OX}})}{RT + \xi_{\text{OX}}\theta_{\text{OX}}(1 - \theta_{\text{OX}})}, \tag{12}$$

with ξ_{OX} being the lateral interaction coefficient in Langmuir adsorption isotherm. Eq.(11) indicates that C_{dl} is negative when $\chi_{\text{OX}} > 1$.

C_{dl}^{Bockris} is the double layer capacitance of the Bockris model,

$$\frac{1}{C_{dl}^{\text{Bockris}}} = \frac{1}{C_{dl}^{GCS}} + \frac{1}{C_{\text{wd}}}. \tag{13}$$

Here, C_{wd} is the capacitance of the water dipole layer,

$$C_{\text{wd}} = -\left(\frac{0.6}{\pi\delta_{\text{IHP}}^2 N_{\text{tot}}} + 1\right)\frac{\epsilon_{\text{IHP}}}{\delta_{\text{IHP}}} + \frac{\epsilon_{\text{IHP}}^2 RT}{N_A N_{\text{tot}}\mu_{\text{w}}^2}\cosh^2(X), \tag{14}$$

and C_{dl}^{GCS} is the double layer capacitance of the modified GCS model accounting for ion-size effect.

$$\frac{1}{C_{dl}^{GCS}} = \frac{1}{C_{\text{str}}} + \frac{\lambda_D}{\epsilon^S} \frac{|\tilde{\sigma}^M| \exp\left(\frac{\gamma(\tilde{\sigma}^M)^2}{2}\right)}{\sqrt{\frac{1}{2\gamma}\left(\exp\left(\frac{\gamma(\tilde{\sigma}^M)^2}{2}\right) - 1\right) + 1}}$$
$$\times \left(\frac{2}{\gamma}\left(\exp\left(\frac{\gamma(\tilde{\sigma}^M)^2}{2}\right) - 1\right)\right)^{-\frac{1}{2}}, \tag{15}$$

with the structural capacitance of the Pt-solution interface, defined as

$$\frac{1}{C_{\text{str}}} = \frac{\delta_{\text{OHP}}}{\epsilon_{\text{OHP}}} + \frac{\delta_{\text{IHP}}}{\epsilon_{\text{IHP}}}. \tag{16}$$

Herein, we assume that the contribution of the adsorbed oxide to the structural capacitance is minor.

Results and discussion

Model parameters, inherited from our previous study with some modifications,[8] are tabulated in Table A1. Figure 2 (a) compares surface charging relations of Pt derived from the GCS model, the Bockris model, and the refined structural model presented in this study with $\gamma = 0$. Figure 2 (b) shows the double-layer capacitance. Both the GCS and Bockris model exhibit an approximately linear charging relation, which can be well described using the classical charging relation based on the pzc concept. The refined structural model of the present study exhibits a non-monotonic charging behaviour with a decrease in σ^M at high ϕ^M, which can be ascribed to impact of the surface oxide dipole. This peculiar charging relation is consistent with experiments of Frumkin and Petrii[4] and Garcia-Araez et al.[6] and DFT studies.[23]
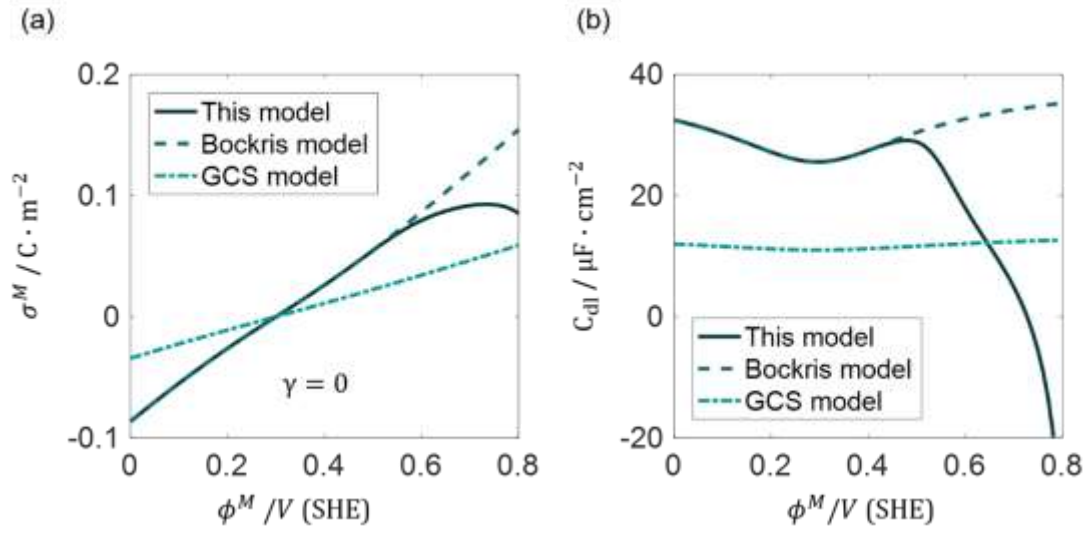
Figure 2. Comparison between Gouy-Chapman-Stern (GCS) model, Bockris model, and the refined structural model of electrified interfaces presented in this study, in terms of (a) surface charging relation and (b) double layer capacitance of a Pt(111) electrode in 0.1 M $HClO_4$ at 25°C. $\gamma = 0$, and other model parameters are given in Table A1.

Figure 2 (b) displays double-layer capacitance of different models. Double-layer capacitance of the GCS model, C_{dl}^{GCS}, slightly changes with varying ϕ^M, and it exhibits the Gouy-Chapman minimum at $\phi^M = \Delta\phi^M$. Double-layer capacitance of the Bockris model, $C_{dl}^{Bockris}$, shows a similar behaviour as the GCS model, except that $C_{dl}^{Bockris}$ is larger than C_{dl}^{GCS}, because of contribution of the ordered water layer. Specifically, at a given σ^M, potential difference across the interface in the Bockris model has a smaller magnitude than that in the GCS model due to the buffering effect exerted by interfacial water molecules.[8, 24] Consequently, $C_{dl}^{Bockris} > C_{dl}^{GCS}$. It is noted that the Gouy-Chapman minimum disappears and evolves into a maximum when γ increases, as shown in Figure 3(a) and already elucidated in ref 12. C_{dl} derived from the refined structural model

10

agrees with C_{dl}^{Bockris} in the low potential range without formation of chemisorbed oxygen species. However, at high potentials C_{dl} decreases relative to C_{dl}^{Bockris} and even assumes negative values when $\phi^M > 0.7\ V$. C_{dl} goes through a maximum at $\phi^M \sim 0.5\ V$, where $\phi_{OHP} = 0.05\ V$.

Kornyshev predicted bell or camel shaped capacitance-potential curves using a modified PB equation, which is reproduced in Figure 3(a).[12] Two symmetrical maxima due to the size effect are observed on the bell-shaped curve for a symmetrical electrolyte. However, in our case, the capacitance maximum at $\phi^M \sim 0.5\ V$ in Figure 2 (b) is not caused by the crowding of counterions, as the compacity is $\gamma = 0$ in Figure 2. This peculiar capacitance maximum is ascribed to the surface oxide dipole formed on the Pt surface.

Ion size effects on C_{dl} derived from this model are shown in Figure 3(b). The maximum due to the surface oxide dipole disappears when γ increases to 0.5, implying that it is easier to observe this maximum in dilute solution. In the Kornyshev formalism, the capacitance-potential curve of a symmetrical electrolyte preserves symmetry around the pzc. Asymmetry can be introduced by accounting for different sizes and charge numbers of anions and cations. The model presented in this study unravels another kind of asymmetry in the capacitance-potential curve that is caused by asymmetry in the specific adsorption behaviour.
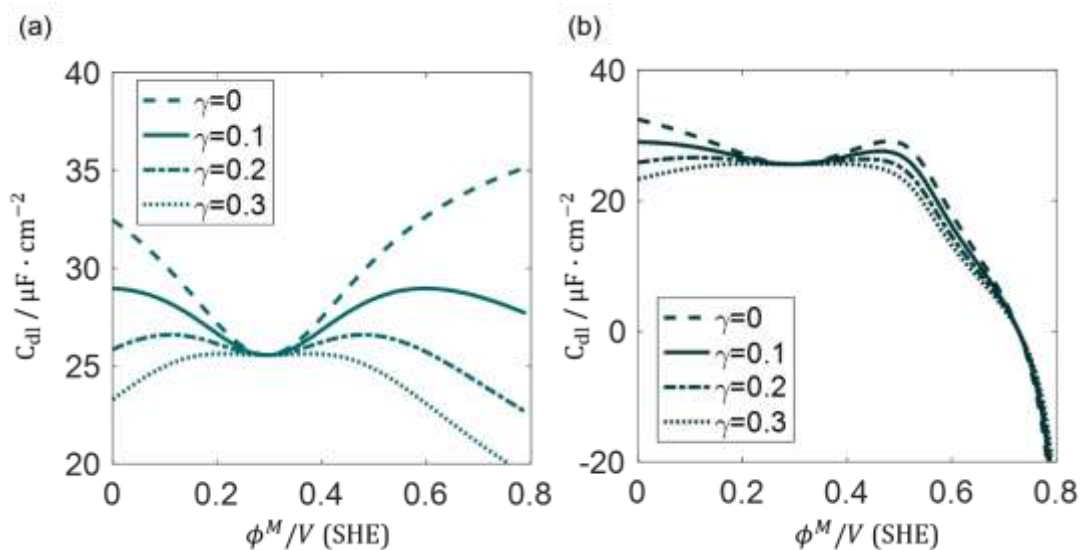
Figure 3. Ion size effect on the double layer capacitance of a Pt(111) electrode in 0.1 M HClO₄ at 25°C calculated using (a) the Bockris model and (b) the presented model.

Pajkossy and Kolb employed EIS to determine the C_{dl} of Pt (111) and Pt (100) electrodes in various of 0.1 M electrolyte solutions.[14, 15] The measured C_{dl} versus ϕ^M curves exhibited a maximum in the potential range of ~0.5 V (SHE) for both electrodes regardless of variations in solute chemistry or solution pH. The authors tentatively correlated the maximum with the pzc, and conjectured that the Gouy-Chapman theory fails in solutions with a concentration exceeding 0.1 M. To prove or disprove this hypothesis, they lowered the solution concentration to 1 mM in a subsequent study.[16] At such a low solute concentration, they expected that the C_{dl} versus ϕ^M curve would show a Gouy-Chapman minimum. However, the maximum still showed, see Figure 4. They concluded that this phenomenon cannot be attributed to the pzc, but that it might be related to changes in the orientation of water molecules at the Pt-solution interface.

However, this explanation is at odds with the Bockris model that considers surficial water molecules but does not produce a capacitance maximum, as seen in Figure 2(b). Another salient feature is that C_{dl} decreases as ϕ^M increases from 0.4 V to 0.6 V (SHE), where the formation of chemisorbed oxygen species progresses, as revealed by Pajkossy and Kolb using the EIS method, and also by Garcia-Araez et al. who developed a thermodynamic approach to determine C_{dl}.[6] The model presented in this article qualitatively reproduces both features, the capacitance maximum at ~0.4 V and the decreasing trend in C_{dl} with increasing ϕ^M in the potential range of 0.4–0.6 V, as shown in Figure 4. We find that the location of the Gouy-Chapman minimum and the surface-oxide related maximum are dictated by $\Delta\phi^M$ and E_{OX}^0, which are adjusted to E_{OX}^0=0.8 V, $\Delta\phi^M$=0.15 V in Figure 4, respectively,. Noticeable deviation between model and experiment is found regarding the ratio between the maximum and the minimum. Experimental data show a steeper transition from the minimum to the maximum. In this regard, parametric analysis reveals that the buffering effect exerted by interfacial water molecules affects. The dashed line corresponding to ten water molecules per Pt sites, namely a stronger buffering effect, shows a steeper transition. The agreement between model and experiment can be improved by employing an explicit treatment of solvent molecules, as in ref 25.
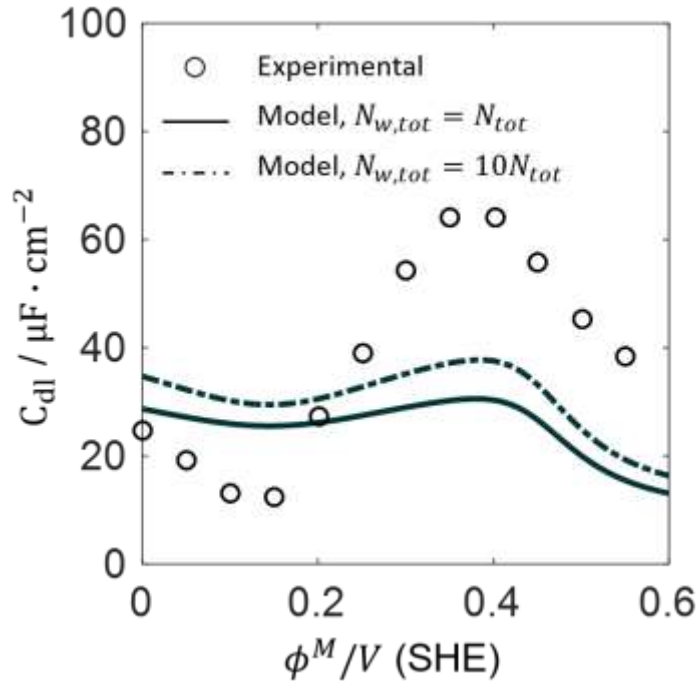
Figure 4. Comparison between model and experiment of double layer capacitance of a Pt(111) electrode in 0.1 mM HClO$_4$ + 0.1 M KClO$_4$ at 25°C. Adjusted model parameters are: E_{OX}^0=0.8 V, $\Delta\phi^M$=0.15 V, and the number of water molecules per Pt site (one for the solid line and ten for the dashed line).

The partial charge number ζ is a key interfacial property that can be determined conveniently by DFT studies. Figure 5 (a) indicates that a larger ζ, namely a greater surface oxide dipole, decreases σ^M to more negative values in the high potential range, leading to a more negative C_{dl}. Moreover, the maximum in C_{dl} occurs at higher ϕ^M when ζ decreases. Figure 5 (b) display the pH effect on C_{dl}. At higher pH, the oxide formation commences at lower potentials, decreasing σ^M to more negative values. The present version of the theory does not produce this behaviour since it does

14

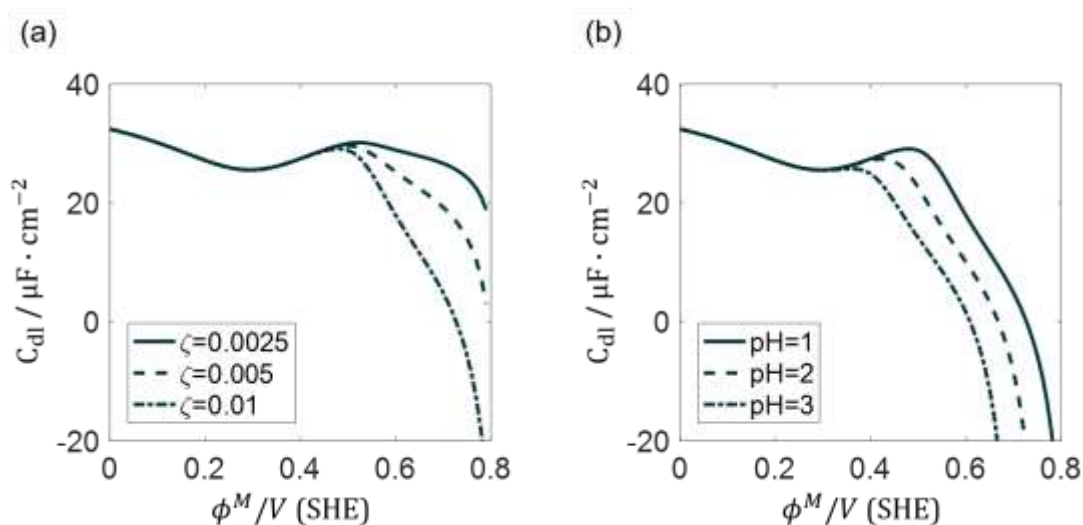not treat the phenomenon of oxide growth and its impact on the metal surface charging phenomenon.[26]

Figure 5. Effect of (a) the partial charge number, ζ, of the oxide layer and (b) the pH on the double layer capacitance a Pt(111) electrode in x M $HClO_4 + (0.1 - x)$ M $KClO_4$ at 25°C. $\gamma = 0$.

Conclusion

In summary, the refined structural model of electrified interfaces that incorporates the formation of chemisorbed oxygen species and a layer of oriented water molecules has been improved by taking into account ion size effects. Moreover, an explicit expression for the double layer capacitance has been derived. Compared with the Gouy-Chapman-Stern and Bockris model, the presented model gives rise to a non-monotonic surface charging relation and a peculiar maximum on the double layer capacitance curve due to the Pt oxidation. Parametric analysis reveals that the oxide-induced capacitance maximum disappears when the ion size coefficient γ grows as a consequence of the increase in solute concentration.

15

Acknowledgement

Appendix

A1. Metal surface charging relation of Bockris and GCS model

The metal charging relation derived from the Bockris model that doesn't consider the surface oxide layer is given by,

$$
\begin{aligned}
\operatorname{sgn}(\sigma^M) \frac{2RT}{F} &\times \operatorname{arsinh}\left(\sqrt{\frac{1}{2\gamma}\left(\exp\left(\frac{\gamma}{2}(\tilde{\sigma}^M)^2\right) - 1\right)}\right) \\
&+ \sigma^M\left(\frac{\delta_{\text{OHP}}}{\epsilon_{\text{OHP}}} + \frac{\delta_{\text{IHP}}}{\epsilon_{\text{IHP}}}\right) \\
&= \left(\phi^M - \phi^S_{\text{bulk}}\right) - \Delta\phi^M + \frac{N_{\text{tot}}\mu_{\text{w}}}{\epsilon_{\text{IHP}}} \cdot \tanh(X),
\end{aligned} \tag{A1}
$$

and that derived from the GCS model that does not account for neither the surface oxide layer nor the surface water molecule layer is given by,

$$
\begin{aligned}
\operatorname{sgn}(\sigma^M) \frac{2RT}{F} &\times \operatorname{arsinh}\left(\sqrt{\frac{1}{2\gamma}\left(\exp\left(\frac{\gamma}{2}(\tilde{\sigma}^M)^2\right) - 1\right)}\right) \\
&+ \sigma^M\left(\frac{\delta_{\text{OHP}}}{\epsilon_{\text{OHP}}} + \frac{\delta_{\text{IHP}}}{\epsilon_{\text{IHP}}}\right) = \left(\phi^M - \phi^S_{\text{bulk}}\right) - \Delta\phi^M.
\end{aligned} \tag{A2}
$$

Note that both the Bockris and GCS model have been improved over their original form by accounting for the ion size effect.

A2. List of model parameters

Tabel A1. Model parameters

Category	Item	Value
Constant	Gas constant, R	8.314 J K^{-1} mol^{-1}
	Faraday constant, F	96485 C mol^{-1}
	Temperature, T	298.15 K
	Elementary charge, e	1.60217662 $\times$ 10^{-19} C
	Avogadro's number, N_A	6.02×10^{23} mol^{-1}
	Water dipole moment, μ_w	3.1 D
	Dissociation constant of water, K_w	1×10^{-8} mol^2 m^{-6}
	Concentration of liquid water, c_l	5.5×10^4 mol m^{-3}
	Pt atom density, N_{tot}	1.5×10^{19} m^{-2}
	Vacuum permittivity, ε_0	8.85×10^{-11} F m^{-1}
Hydrogen adsorption and Oxide formation	Equilibrium potential of hydrogen adsorption, E_{Had}^0	0.3737 V
	Lateral interaction parameter of H adsorption, ξ_{Had}	29.2 kJ mol^{-1}
	Index of Pt oxidation mechanism, υ	1
	Equilibrium potential of Pt oxidation, E_{OX}^0	0.716 V
	Lateral interaction parameter of oxide adsorption, ξ_{OX}	64.2(1-θ_{OX}) kJ mol^{-1}
Parameters of the interface	Permittivity of the oxide layer, ε_{PtO}	1 ε_0
	Permittivity of the IHP, ε_{IHP}	6 ε_0
	Permittivity of the IHP, ε_{OHP}	30 ε_0
	Permittivity of bulk water, ε^S	78.5 ε_0
	Effective thickness of the oxide layer, δ_{PtO}	0.2 nm
	Charge number of oxide dipole, ς	0.01
	Thickness of the IHP, δ_{IHP}	0.275 nm
	Thickness of the OHP, δ_{OHP}	0.515 nm
	Potential drop at Pt surface, $\Delta\phi^M$	0.3 V

In our previous work, we assumed that $\epsilon_{PtO} = 30\epsilon_0$ based on dielectric constants of bulk metal oxides.[8] However, one should note that there is nothing but vacuum between Pt and O_{ad} atoms in the monolayer. As a result, $\epsilon_{PtO} = 1$, should be used for the medium between Pt and O_{ad} atoms. In addition, we used $\varsigma = 0.8$, based on our previous DFT calculation of the surface oxide dipole.[8] However, a more recent

comprehensive DFT studies of chemisorbed oxygen on Pt(111) shows that the surface oxide dipole is much smaller.[23] As a result, we used a new value of 0.01 in this work.

Reference

1. A. N. Frumkin, O. A. Petrii and B. B. Damaskin, in *Comprehensive Treatise of Electrochemistry: The Double Layer*, edited by J. O. M. Bockris, B. E. Conway and E. Yeager (Springer US, Boston, MA, 1980), pp. 221-289.

2. S. Trasatti and E. Lust, in *Modern Aspects of Electrochemistry*, edited by R. E. White, J. O. M. Bockris and B. E. Conway (Springer US, Boston, MA, 1999), pp. 1-215.

3. A. Frumkin and A. Gorodetzkaja, Z. Phys. Chem. **136**, 451-472 (1928).

4. A. N. Frumkin and O. A. Petrii, Electrochimica Acta **20** (5), 347-359 (1975).

5. O. A. Petrii, Russian Journal of Electrochemistry **49** (5), 401-422 (2013).

6. N. Garcia-Araez, V. Climent, E. Herrero, J. M. Feliu and J. Lipkowski, Electrochimica Acta **51** (18), 3787-3793 (2006).

7. M. J. Eslamibidgoli, J. Huang, T. Kadyk, A. Malek and M. Eikerling, Nano Energy **29**, 334-361 (2016).

8. J. Huang, A. Malek, J. Zhang and M. H. Eikerling, The Journal of Physical Chemistry C **120** (25), 13587-13595 (2016).

9. I. Borukhov, D. Andelman and H. Orland, Physical Review Letters **79** (3), 435-438 (1997).

10. M. Z. Bazant, B. D. Storey and A. A. Kornyshev, Physical Review Letters **106** (4), 046102 (2011).

11. D. Gillespie, Microfluidics and Nanofluidics **18** (5), 717-738 (2015).

12. A. A. Kornyshev, The Journal of Physical Chemistry B **111** (20), 5545-5557 (2007).

13. J. J. Bikerman, The London, Edinburgh, and Dublin Philosophical Magazine and Journal of Science **33** (220), 384-397 (1942).

14. T. Pajkossy and D. M. Kolb, Electrochimica Acta **46** (20), 3063-3071 (2001).

15. Z. Kerner, T. Pajkossy, L. A. Kibler and D. M. Kolb, Electrochemistry Communications **4** (10), 787-789 (2002).

16. T. Pajkossy and D. M. Kolb, Electrochemistry Communications **5** (4), 283-285 (2003).

17. M. Gouy, J. Phys. Theor. Appl. **9** (1), 457-468 (1910).

18. D. L. Chapman, Philosophical Magazine **25** (148), 475-481 (1913).

19. H. V. Helmholtz, Annalen der Physik **243** (7), 337-382 (1879).

20. H. von Helmholtz, Ann. Phys **165**, 211-233 (1853).

21. O. Stern, Berichte der Bunsengesellschaft für physikalische Chemie **30** (21 - 22), 508-516 (1924).

22. W. Schmickler and E. Santos, *Interfacial Electrochemistry*. (Springer Science & Business Media, 2010).

23. A. Malek and M. Eikerling, Electrocatalysis (2017). https://doi.org/10.1007/s12678-017-0436-0.

24. J. M. Bockris, M. A. Devanathan and K. Muller, Proceedings of the Royal Society of London. Series A. Mathematical and Physical Sciences **274** (1356), 55 (1963).

25 M. Landstorfer, C.Guhlke, and W.Dreyer, Electrochimica Acta **201**, 187–219 (2016).

26. H. A. Baroody, G. Jerkiewicz and M. H. Eikerling, The Journal of Chemical Physics **146** (14), 144102 (2017).